

## Spectroscopic analyses on the binding interaction of thiosemicarbazone-derived Cu(II) complex with DNA/BSA

Mükerrem Fındık<sup>1\*</sup> , Asuman Uçar<sup>2</sup> , Emine Güler Akgemci<sup>3</sup> 

<sup>1</sup> Necmettin Erbakan University, A.K. Education Faculty, Department of Chemistry Education, Research Laboratory, Konya, Turkey

<sup>2</sup> Agri Ibrahim Cecen University, Education Faculty, Department of Science Education, Ağrı, Turkey

<sup>3</sup> Necmettin Erbakan University, A.K. Education Faculty, Department of Chemistry Education, Konya, Turkey

\* [mmukerrem@gmail.com](mailto:mmukerrem@gmail.com)

\*Orcid: 0000-0002-9441-0814

Received: 30 March 2021

Accepted: 1 June 2021

DOI: 10.18466/cbayarfbe.902377

### Abstract

Cu(II) complex of 2-hydroxy-5-methoxyacetophenone-N(4)-ethyl thiosemicarbazone (Cu(HMAET)Cl) was synthesized and characterized by spectroscopic methods such as FT-IR, <sup>1</sup>H-NMR and UV-Vis. The Cu(II) complex's DNA-binding capacity was studied with the UV-Vis absorption titration and ethidium bromide (EB) displacement experiment using *E. coli* DNA. The results demonstrated that the Cu(II) complex could intercalate in the DNA's base pairs. The binding constant was found as  $2.8 \times 10^7 \text{ M}^{-1}$ . Also, the interaction study of the Cu(II) complex with bovine serum albumin (BSA) was investigated using the UV-Vis absorption and fluorescence spectroscopy techniques. It was concluded that the Cu(II) complex interacts strongly with BSA.

**Keywords:** Thiosemicarbazone, copper(II) complex, DNA/BSA binding, fluorescence quenching, absorption

### 1. Introduction

Studies on the interaction of DNA and small molecules, which are of great importance in human life, are important for developing new pharmaceutical molecules [1-3]. DNA is an important intracellular target for anticancer drugs as it regulates most biochemical processes occurring in cellular systems [4-6]. Therefore, a drug should be designed to bind specifically to DNA. Generally, complexes interact with DNA by intercalating between base pairs or binding to the grooves of the DNA. These non-covalent binding modes' weak interactions are reversible and less toxic to healthy cells [7]. Therefore, it is very important to prepare such metal complexes.

Researchers know that Cu(II) complexes, which have a wide range of biological activity, show anti-inflammatory, antiviral, and antitumor properties [3,8,9]. It has been observed that the presence of copper ions in the complexes increases the effectiveness of the drug and organic therapeutic agents [10]. Besides, Cu(II) complexes can lead to oxidative cleavage of DNA by means of chemical oxidants [11]. In the last ten years, many Cu(II) complexes with strong DNA binding

and cutting ability have been synthesized. Most of them show excellent anticancer and apoptosis regulating effects [12,13]. Cu(II) complexes are also promising in preparing less toxic anticancer drugs [14-16]. Recently, many researchers have been working on the interaction between Cu(II) complexes and serum albumin, such as Human serum albumin (HSA)/bovine serum albumin (BSA), because proteins, like DNA, are also targets of anticancer drugs [7,17]. HSA and BSA are the most abundant carrier proteins in animal plasma [18]. BSA is often chosen as a model protein because of its structural similarity with HSA, has the advantages of low cost, high stability, good water solubility, wide availability, and easy binding with different compounds [17,19].

Therefore, in this study, the thiosemicarbazone-derived Cu(II) complex was synthesized and investigated the binding interaction with DNA and BSA using UV-Vis absorption and fluorescence spectroscopy techniques.

### 2. Materials and Methods

#### 2.1. Chemicals and Apparatus

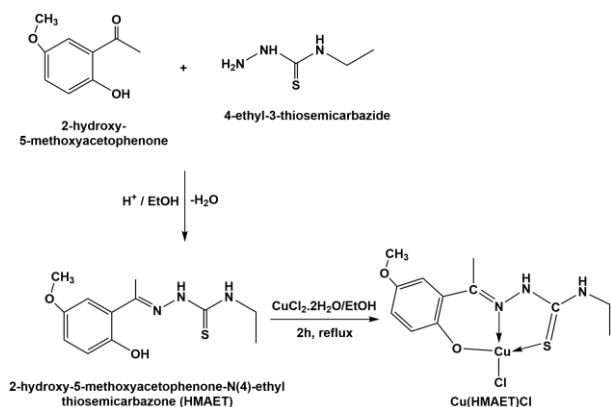
4-Ethyl-3-thiosemicarbazide, 2-hydroxy-5-methoxyacetophenone, bovine serum albumin (BSA),

ethidium bromide (EB), copper(II) chloride dihydrate ( $\text{CuCl}_2 \cdot 2\text{H}_2\text{O}$ ) and sodium chloride (NaCl) were purchased from Sigma Aldrich. Ethyl alcohol (EtOH) and N,N-dimethylformamide (DMF) were obtained from Merck.

Perkin-Elmer 2400 CHN elemental analyzer was used for elemental analysis (C, H, and N) of the sample. A Bruker AC 400 (400 MHz) NMR spectrometer was used to record the  $^1\text{H}$ -NMR spectrum. Perkin-Elmer Spectrum 100 with Universal ATR Polarization Accessory (Shelton, USA) was used for the FT-IR spectrum. Absorbance spectra were monitored by Shimadzu UV-1800 double beam spectrophotometer. Fluorescence spectra were obtained using a PTI Quantmaster 400 Fluorometer spectrophotometer.

## 2.2. Synthesis of HMAET and Cu(HMAET)Cl

HMAET and Cu(HMAET)Cl was synthesized from the previous study by following the related procedure: HMAET; equimolar solutions of 2-hydroxy-5-methoxyacetophenone and 4-ethyl-3-thiosemicarbazide were dissolved in 30 mL of absolute EtOH and 2-3 drops of conc.  $\text{H}_2\text{SO}_4$  was added. The mixture was stirred for 2 h at room temperature. The resulting solid was filtered and recrystallized twice with an EtOH/water mixture. Cu(HMAET)Cl; 1.5 mmol of the HMAET was dissolved in EtOH (30 mL) with gentle heating. An equimolar amount of  $\text{CuCl}_2 \cdot 2\text{H}_2\text{O}$  was dissolved in the minimum quantity of the same solvent and added dropwise to the HMAET solution. The mixture was refluxed for approximately 2 h, and then slowly evaporated at  $35^\circ\text{C}$  until sufficient solid formed. The resulting solid was filtered and washed with anhydrous ether [20,21].



**Scheme 1.** Synthesis of Cu(HMAET)Cl.

The synthesis procedure of the ligand and complex is given in the Scheme 1. Dark green crystals, yield 67.5 %; mp:  $153\text{--}154^\circ\text{C}$ . Anal. calc. ( $\text{C}_{12}\text{H}_{15}\text{ClCuN}_3\text{O}_2\text{S}$ ); C, 39.56; H, 4.15; N, 11.53; S, 8.80 %. Found: C, 39.59; H, 4.17; N, 11.56; S, 8.91 %.  $^1\text{H}$ -NMR (400 MHz, DMSO- $d_6$ ):  $\delta$  (ppm): 8.74 (s, 1H, -NH), 6.82 (s, 1H,  $\text{H}_{\text{Ar}}$ ), 6.98

(d, 2H,  $\text{H}_{\text{Ar}}$ ), 3.81 (s, 3H, - $\text{OCH}_3$ ), 3.78 (m, 2H, - $\text{CH}_2$ ), 2.38 (s, 3H, - $\text{CH}_3$ ), 1.31 (t, 3H, - $\text{CH}_3$ ). FT-IR ( $\text{cm}^{-1}$ ): 3442, 3261, 1626, 1568, 1523, 1260, 1217, 1036, 823, 778, 526, 443, 315, 284, 179.

## 2.3. DNA binding study

The *E. coli* DNA binding experiments of Cu(HMAET)Cl were investigated using a UV-Vis spectrometer. Absorbance measurements were obtained with different concentrations of *E. coli* DNA (0.1–1.4  $\mu\text{M}$ ) in distilled water with Tris-HCl buffer (5 mM Tris/50 mM NaCl, pH 7.2) by adding to the Cu(HMAET)Cl (50  $\mu\text{M}$  in DMF).

## 2.4. Displacement experiment with EB

Displacement experiments of EB were studied by fluorescence spectroscopy. Interaction has been recorded by the gradual addition of different concentrations of Cu(HMAET)Cl to Tris-HCl buffer (5 mM Tris/50 mM NaCl, pH 7.2) solution of EB-DNA (10  $\mu\text{M}$ ). The measurements were recorded after waiting half an hour.

## 2.5. Interaction with BSA

Fluorescence spectra measurements were recorded in phosphate-buffered saline (PBS) at pH 7.5 to study the interaction of Cu(HMAET)Cl with BSA. The emission spectra were initially monitored using 2 mL of BSA solution (1  $\mu\text{M}$ ), following the incremental additions (0–2.5  $\mu\text{M}$ ) of Cu(HMAET)Cl. In addition, the absorbance measurement of BSA solution (10  $\mu\text{M}$  in PBS) was investigated in the presence and the absence of Cu(HMAET)Cl (4  $\mu\text{M}$  in DMF).

## 2.6. Statistical analysis

For statistical analysis, experiments were run in triplicate. Plots were prepared according to the average.

## 3. Results and Discussion

### 3.1. Characterizations of Cu(HMAET)Cl

The FT-IR spectrum of Cu(HMAET)Cl (Figure 1) showed a band at  $3261\text{ cm}^{-1}$ , which is attributed to the  $\nu(\text{N-H})$  band [22]. It was seen that  $\nu(\text{C=N})$  and  $\nu(\text{N-N})$  bands peaked at  $1523\text{ cm}^{-1}$  and  $1036\text{ cm}^{-1}$ , respectively [23,24]. Vibrations of  $\nu(\text{C-S})$  which became from  $\nu(\text{C=S})$  bond after coordination occurred at  $823\text{ cm}^{-1}$  [25]. The bands observed at 179, 315, 443 and  $526\text{ cm}^{-1}$  are  $\nu(\text{Cu-Cl})$ ,  $\nu(\text{Cu-S})$ ,  $\nu(\text{Cu-N})$  and  $\nu(\text{Cu-O})$  bonds, respectively, indicating the formation of the Cu(II) complex.

The  $^1\text{H}$ -NMR spectrum of Cu(HMAET)Cl was monitored in DMSO- $d_6$  solvent (Figure 2). The signals at 1.31 ppm correspond to the methylene protons of the ethyl group, whilst the  $-\text{CH}_2$  protons of the ethyl group appeared as a multiplet at 3.78 ppm [26,27]. The singlet assigned to  $-\text{CH}_3$  of the azomethine group occurred at

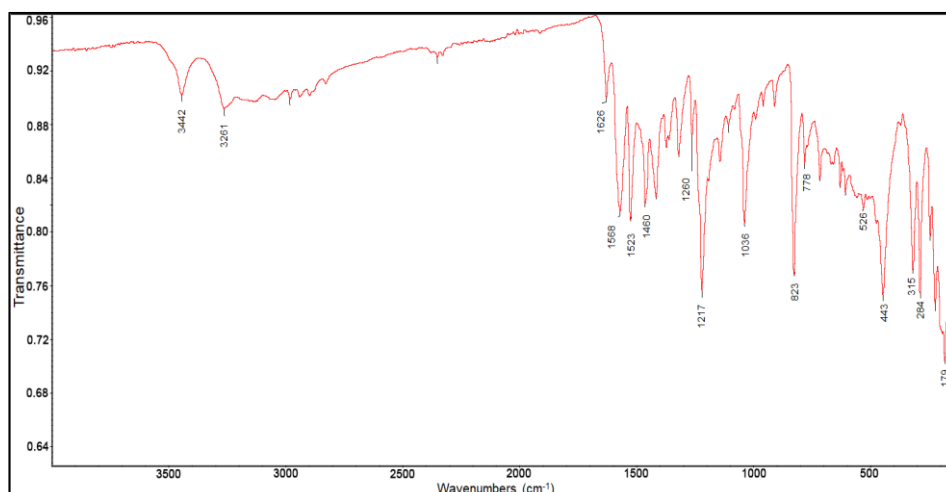


Figure 1. FT-IR spectrum of Cu(HMAET)Cl.

2.38 ppm [28]. A singlet corresponding to the  $-OCH_3$  group was observed at 3.81 ppm [29]. The aromatic protons showed signals at 6.82 and 6.98 ppm. The thiocarbonyl attached  $-NH$  proton was observed at 8.74 ppm.

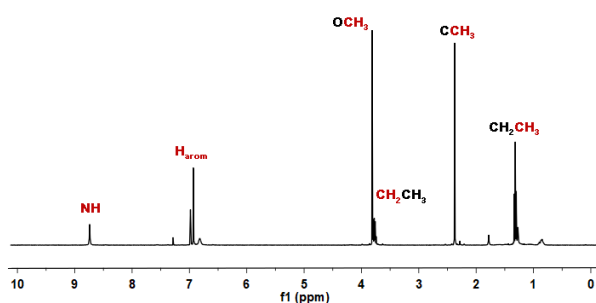


Figure 2.  $^1H$ -NMR spectrum of Cu(HMAET)Cl.

The electronic spectrum was monitored in DMF in the 235–465 nm region at room temperature (Figure 3). Cu(HMAET)Cl showed intraligand transitions at 310 and 265 nm attributed to  $n/\pi^*$  and  $\pi/\pi^*$  transitions, respectively [39]. The band at 370 nm corresponding to the ligand to metal charge transfer transitions [31] can be the evidence of the combination of  $S \rightarrow Cu$ ,  $N \rightarrow Cu$ ,  $O \rightarrow Cu$ , and the ligand to metal charge transfer transition (LMCT) [32].

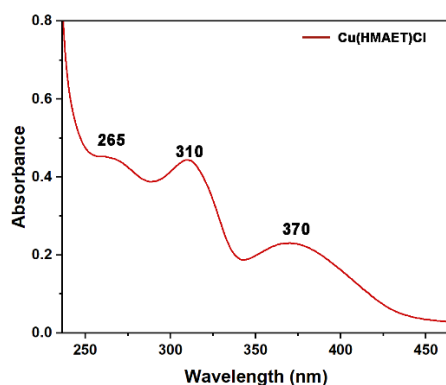


Figure 3. UV-Vis spectrum of Cu(HMAET)Cl.

## 3.2. DNA binding experiments

### 3.2.1. UV absorption spectra of DNA

Interaction studies of DNA and metal complexes are important for understanding the mechanism of interaction and designing effective chemotherapeutic agents and new anticancer drugs [33–35]. UV-Visible absorption titration experiment was performed to examine the Cu(II) complex and *E. coli* DNA binding interaction. Figure 4A shows the absorption spectra of the Cu(II) complex in the presence and absence of *E. coli* DNA. Absorption titration was carried out by adding different concentrations of *E. coli* DNA (0.1–1.4  $\mu M$ ; 5 mM Tris-HCl/50 mM NaCl, pH:7.2) to the Cu(II) complex (50  $\mu M$ ). After increasing the amount of *E. coli* DNA to the Cu(II) complex, the spectrum showed a hypochromism of about 5 %, 15 %, and 9 % with a blue shift of 6, 3, and 22 nm at 282, 324, and 408 nm. According to the results obtained, the binding to *E. coli* DNA was confirmed from the Cu(II) complex's absorption changes. The amount of binding interaction between *E. coli* DNA and the Cu(II) complex was described using the binding constant  $K_b$ , which is calculated from Eq. (1) [36,37].

$$\frac{[DNA]}{(\varepsilon_a - \varepsilon_f)} = \frac{[DNA]}{(\varepsilon_b - \varepsilon_f)} + \frac{1}{K_b(\varepsilon_b - \varepsilon_f)} \quad (1)$$

Where [DNA] is the concentration of *E. coli* DNA,  $\varepsilon_f$ ,  $\varepsilon_a$ , and  $\varepsilon_b$  correspond to the extinction coefficient for the free complex,  $A_{obsd}/[complex]$ , and the extinction coefficient for the complex in the fully bound form, respectively.  $K_b$  was found by calculating the ratio of slope/intercept in the linear plot of  $[DNA]/(\varepsilon_a - \varepsilon_f)$  vs. [DNA] (Figure 4B). The binding constant ( $K_b$ ) value for the interaction of the Cu(II) complex with *E. coli* DNA was found as  $2.8 \times 10^7 M^{-1}$ . The  $K_b$  value of the Cu(II) complex confirms that it binds to the DNA helix via the intercalative mode [11,34,36].

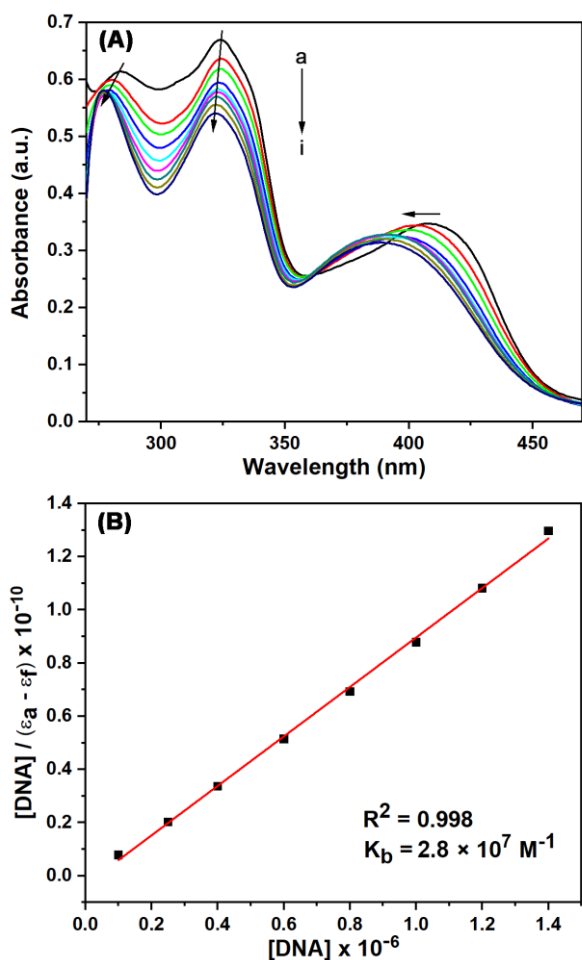


**Figure 4.** (A) Absorption spectrum of Cu(HMAET)Cl (50  $\mu\text{M}$ ) at various concentrations of *E. coli* DNA: a) 0.0  $\mu\text{M}$ ; b) 0.1  $\mu\text{M}$ ; c) 0.25  $\mu\text{M}$ ; d) 0.4  $\mu\text{M}$ ; e) 0.6  $\mu\text{M}$ ; f) 0.8  $\mu\text{M}$ ; g) 1.2  $\mu\text{M}$ ; h) 1.4  $\mu\text{M}$ . (B) The plot of  $[\text{DNA}]/(\epsilon_a - \epsilon_f)$  vs.  $[\text{DNA}]$  for the titration of Cu(HMAET)Cl with *E. coli* DNA.

### 3.2.2. Ethidium Bromide (EB) Displacement

Known as an intercalator, EB can intercalate into double-stranded DNA. Free EB and DNA have very weak fluorescence. When EB intercalates the double-stranded DNA, the fluorescence intensity of the compound becomes extremely strong. However, by intercalating some compounds to DNA, the DNA binding sites of EB are decreased, causing the fluorescence of the EB-DNA system to be quenched [10,11,38]. EB displacement assay for the Cu(II) complex was performed by fluorescence method. The study was carried out by titration of the Cu(II) complex varying between 2.5 and 11.5  $\mu\text{M}$  into 10  $\mu\text{M}$  DNA and 10  $\mu\text{M}$  EB solution. After adding each aliquot, the emission spectra of the DNA-EB complex, which was applied as an excitation wavelength of 540 nm, were recorded between 550 nm and 760 nm. The fluorescence spectra of the DNA-EB in the presence and absence of the Cu(II) complex (Figure 5A) show that

the fluorescence intensity of DNA-EB is quenched significantly in each addition with increasing amounts of the Cu(II) complex. This result indicated that the Cu(II) complex was able to replace EB in the DNA helix. Thus the Cu(II) complex can bind to DNA via intercalative binding mode. The Stern–Volmer (S-V) constant was used for the quenching efficiency of the Cu(II) complex [39],

$$F^0/F = 1 + K_{SV} [Q] \quad (2)$$

where  $F/F^0$ ,  $K_{SV}$ ,  $[Q]$  are the fluorescence intensities in the presence/absence of the Cu(II) complex, the linear S-V quenching constant, and concentration of the Cu(II) complex, respectively. The  $K_{SV}$  value is calculated from the ratio of slope/intercept in the linear plot of  $[Q]$  vs.  $F^0/F$  and is found to be  $2.8 \times 10^6 \text{ M}^{-1}$  (Figure 5B).

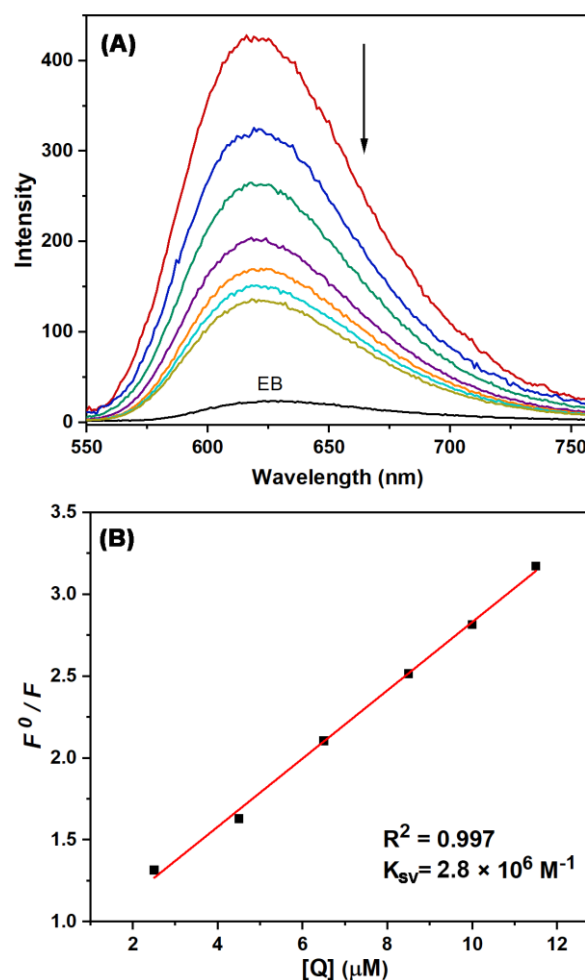


**Figure 5.** (A) Fluorescent quenching with increasing Cu(HMAET)Cl to DNA/EB Conditions:  $[\text{EB}] = 10 \mu\text{M}$ ,  $[\text{DNA}] = 10 \mu\text{M}$ ,  $[\text{Cu(II) complex}] = 2.5\text{--}11.5 \mu\text{M}$ . (B) S-V plot of fluorescence titrations of Cu(HMAET)Cl with *E. coli* DNA.

### 3.3. BSA binding experiments

#### 3.3.1. Fluorescence Quenching of BSA

One of the most effective techniques used to study interactions between compounds and BSA is fluorescence spectroscopy.

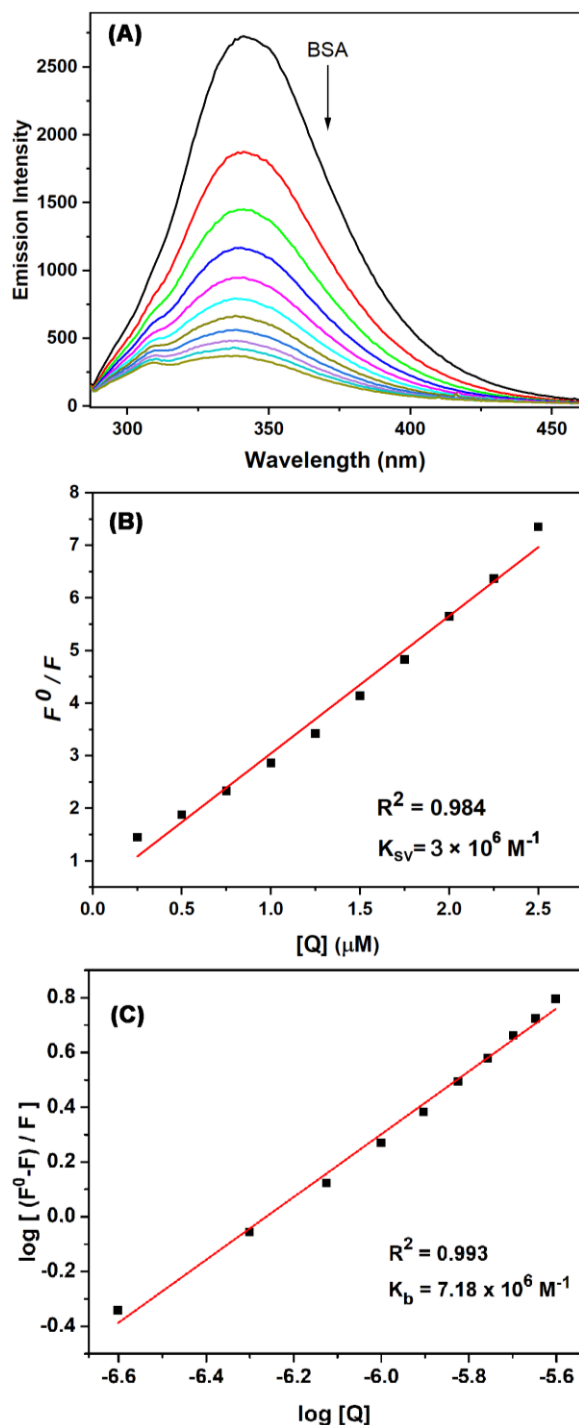


**Figure 6.** (A) Fluorescence quenching of BSA (1  $\mu\text{M}$ ;  $\lambda_{\text{ex}}=280$ ;  $\lambda_{\text{em}}=341$  nm) in presence/absence of various concentrations of Cu(HMAET)Cl (0–2.5  $\mu\text{M}$ ); (B) S-V plot of Cu(HMAET)Cl with BSA; (C) Scatchard plot of Cu(HMAET)Cl with BSA.

Fluorescence of the BSA is due to the fluorophore groups in its structure, such as tryptophan, tyrosine, and phenylalanine. When any compound interacts with BSA, fluorescence intensity quenches [18,36].

The variations in the BSA fluorescence intensity were noted over the range of 285–460 nm ( $\lambda_{\text{ex}} = 280$  nm) with the incremental addition of the Cu(II) complex (0–2.5  $\mu\text{M}$ ) to a fixed concentration of BSA (1  $\mu\text{M}$ ) prepared in PBS buffer solution (pH = 7.5). The quenching of BSA fluorescence (Figure 6A) with the addition of the Cu(II) complex was observed at  $\lambda = 341$  nm with a percentage of 86.39 %, along with a hypsochromic shift of 6 nm. The main reason for this was that the protein's active sites are embedded in a hydrophobic environment [40,41].

These results showed that the Cu(II) complex had a definite interaction with the BSA protein. The S-V equation has been used to interpret the possible quenching mechanism.

$$\frac{F^0}{F} = 1 + K_q \tau_0 [Q] = 1 + K_{SV} [Q] \quad (3)$$

Where  $F/F^0$ ,  $K_q$ ,  $[Q]$  and  $\tau_0$  the fluorescence intensities in the presence/absence of the complex, the bimolecular quenching rate constant, the concentration of the complex, and the average lifetime ( $10^{-8}$  s) of protein without complex, respectively.  $K_{SV}$  is the S-V quenching constant and is equal to  $K_q \tau_0$ . The value of  $K_{SV}$  was obtained as slope of the linear plot of  $F^0/F$  vs.  $[Q]$  and was found to be  $3 \times 10^6 \text{ M}^{-1}$ . The  $K_q$  was found to be  $3 \times 10^{14} \text{ M}^{-1} \text{ s}^{-1}$  (Figure 6B).

If any molecule binds to BSA's active site, the Scatchard equation is used to calculate the equilibrium binding constant and the number of binding sites [42].

$$\log[(F^0 - F)/F] = \log K_b + n \log [Q] \quad (4)$$

Where  $F/F^0$ ,  $K_b$ , and  $n$  are the fluorescence intensity in the presence/absence of the complex, the binding constant of the complex with BSA, and the number of binding sites. The  $K_b$  and  $n$  were calculated from the intercept and slope in the linear plot of  $\log[(F^0-F)/F]$  vs.  $\log [Q]$ , respectively and was found to be  $7.18 \times 10^6 \text{ M}^{-1}$  and  $n = 1.14$  (Figure 6C). A binding site value close to 1 indicates that there is only one binding site between the Cu(II) complex and BSA. The obtained  $K_q$  and  $K_b$  values prove that there is a strong interaction between the Cu(II) complex and BSA.

#### 3.3.2. UV absorption spectra of BSA

Comparing the characteristic absorption spectra of pure BSA and BSA-complex solutions determines whether the complexes bind to BSA statically or dynamically. Static quenching causes a change in the absorption

**Table 1.** Binding constants for DNA/protein with compounds.

Complex	DNA		BSA/HSA		Ref.
	$K_b (M^{-1})$	$K_{sv} (M^{-1})$	$K_b (M^{-1})$	$K_{sv} (M^{-1})$	
<b>Cu(phen)(H<sub>2</sub>O)L<sub>2</sub></b> <b>Cu(dmphen)L<sub>2</sub></b>	1.4 x 10 <sup>4</sup> 6.4 x 10 <sup>4</sup>	-	-	-	1
<b>[Cu(L<sub>1</sub>)(phen)][Cu(L<sub>1</sub>)(phen)]·5H<sub>2</sub>O</b> <b>[Cu(L<sub>2</sub>)(1,10-phen)](ClO<sub>4</sub>)</b>	-	2.20 x 10 <sup>4</sup> 2.27 x 10 <sup>4</sup>	-	-	8
<b>[Cu(phen)(gln)(H<sub>2</sub>O)]NO<sub>3</sub>·H<sub>2</sub>O</b> <b>[Cu(dmphen)(gln)(H<sub>2</sub>O)]ClO<sub>4</sub></b>	3.62 x 10 <sup>3</sup> 7.33 x 10 <sup>3</sup>	4.40 x 10 <sup>3</sup> 4.26 x 10 <sup>4</sup>	-	- 1.17 x 10 <sup>4</sup>	9
<b>qCuBBPc</b>	2.97 x 10 <sup>5</sup>	1.003 x 10 <sup>5</sup>	-	-	11
<b>H<sub>3</sub>L-Cu</b>	-	-	4.42 x 10 <sup>4</sup>	1.19 x 10 <sup>4</sup>	18
<b>CuL</b>	2.15 x 10 <sup>6</sup>	-	-	-	43
<b>[Cu(H<sub>2</sub>L<sup>1</sup>)(imH)(H<sub>2</sub>O)].3H<sub>2</sub>O</b> <b>[Cu(H<sub>2</sub>L<sup>3</sup>)(imH)<sub>2</sub>].H<sub>2</sub>O</b>	1.76 x 10 <sup>3</sup> 0.85 x 10 <sup>3</sup>	11.73 x 10 <sup>3</sup> 5.42 x 10 <sup>3</sup>	-	10.48 x 10 <sup>3</sup> 29.64 x 10 <sup>3</sup>	44
<b>C<sub>51</sub>H<sub>42</sub>Cu<sub>2</sub>N<sub>4</sub>O<sub>6</sub></b>	4 x 10 <sup>5</sup>	-	-	-	45
<b>Cu<sub>2</sub>(μ<sub>2</sub>-Br)<sub>2</sub>(η<sup>1</sup>-S-9-Hanttc)<sub>2</sub>(Ph<sub>3</sub>P)<sub>2</sub></b>	10.36 x 10 <sup>4</sup>	1.02 x 10 <sup>4</sup>	14.09 x 10 <sup>6</sup>	15.6 x 10 <sup>5</sup>	46
<b>Cu(HMAET)Cl</b>	2.8 x 10 <sup>7</sup>	2.8 x 10 <sup>6</sup>	7.18 x 10 <sup>6</sup>	3 x 10 <sup>6</sup>	<b>This work</b>

spectrum of the fluorophore group with the formation of a new complex-BSA, while no change in the dynamic quenching absorption spectrum is observed. The absorption spectrum of the BSA solution and the Cu(II) complex-BSA was given in Figure 7. The increase in the absorption intensity without any shifting with the addition of the Cu(II) complex (4 μM) on BSA (10 μM) indicates static quenching [34,41,42].

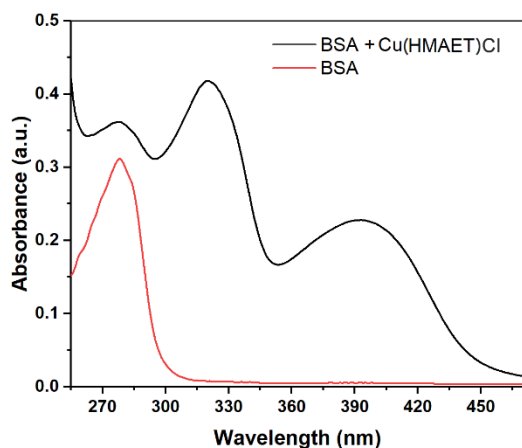


**Figure 7.** Absorption spectrum of BSA (10 μM) and BSA with Cu(HMAET)Cl (4 μM).

#### 4. Conclusion

This paper is containing the synthesis of the the Cu(II) complex of thiosemicarbazone prepared by the combination of 2-hydroxy-5-methoxyacetophenone and

4-ethyl-3-thiosemicarbazide. The Cu(II) complex was characterized by elemental analysis, UV-Vis, FT-IR, and <sup>1</sup>H-NMR spectroscopies. When the spectral changes in the absorption spectra of the Cu(II) complex with increasing *E. coli* DNA addition were examined, hypochromism and small shifts to blue were observed in the Cu(II) complex. The binding constant of the Cu(II) complex with *E. coli* DNA was calculated as 2.8×10<sup>7</sup> M<sup>-1</sup>. The Cu(II) complex exhibits hypochromism and small shifts in blue

wavelength and has a binding constant less than 10<sup>6</sup>, the  $K_b$  value, proving that the Cu(II) complex interacts by intercalating binding to DNA. In the study of displacement with EB performed using fluorescence spectroscopy, which is another important spectroscopic technique that examines the interaction of the Cu(II) complex with DNA, significant reductions in EB-DNA emission intensity were observed with increasing the Cu(II) complex concentration. This result confirms that the Cu(II) complex binds to DNA via the intercalation mechanism. In BSA binding studies, the  $K_b$  value of emission spectroscopy shows considerable interaction between BSA and the Cu(II) complex, while the absorption study has shown that this interaction is by a static quenching mechanism. When the binding interactions of the previously studied copper complexes with both DNA and BSA were evaluated, it was found that the Cu(HMAET)Cl complex had a good binding effect with DNA/BSA (Table 1). It is thought that these results obtained with the Cu(II) complex will be useful in understanding the mechanism of biomolecules and

complexes and in the development of new potential anticancer agents.

### Acknowledgement

The author is grateful to Dr. Suray Pehlivanoglu, Department of Molecular Biology and Genetics, Faculty of Science, Necmettin Erbakan University, Konya, for providing *E. coli* DNA.

### Author's Contributions

Mükerrem FINDIK: Drafted and wrote the manuscript, performed the experiment and result analysis.

Asuman UÇAR: Performed the experiment and result analysis and helped in manuscript preparation.

Emine Güler AKGEMCİ: Assisted in analytical analysis on the structure, supervised the experiment's progress, result interpretation and helped in manuscript preparation.

### Ethics

There are no ethical issues after the publication of this manuscript.

### References

1. Eremina, JA, Lider, EV, Sukhikh, TS, Klyushova, LS, Perepechaeva, ML, Sheven, DG, Berezin, AS, Grishanova, AY, Potkin VI. 2020. Water-soluble copper(II) complexes with 4,5-dichloro-isothiazole-3-carboxylic acid and heterocyclic N-donor ligands: Synthesis, crystal structures, cytotoxicity, and DNA binding study. *Inorganica Chimica Acta*; 510: 119778.
2. Kaya, B, Yılmaz ZK, Şahin, O, Aslim, B, Ülküseven, B. 2020. Structural characterization of new zinc(II) complexes with N<sub>2</sub>O<sub>2</sub> chelating thiosemicarbazidato ligand; Investigation of the relationship between their DNA interaction and in vitro antiproliferative activity on human cancer cells. *New Journal of Chemistry*; 44: 9313-9320.
3. Karami, K, Rahimi, M, Zakariazadeh, M, Buyukgungor, O, Amirghofran, Z. 2018. New phosphorus ylide palladacyclic: Synthesis, characterization, X-Ray crystal structure, biomolecular interaction studies, molecular docking and in vitro cytotoxicity evaluations. *Journal of Organometallic Chemistry*; 878: 60-76.
4. Beebe, SJ, Celestine, MJ, Bullock, JL, Sandhaus, S, Arca, JF, Crokek, DM, Ludvig, TA, Foster, SR, Clark, JS, Beckford, FA, Tano, CM, Tonsel-White, EA, Gurung, RK, Stankavich, CE, Tse-Dinh, YC, Jarrett, WL, Holder, AA. 2020. Synthesis, characterization, DNA binding, topoisomerase inhibition, and apoptosis induction studies of a novel cobalt(III) complex with a thiosemicarbazone ligand. *Journal of Inorganic Biochemistry*; 203: 110907.
5. Milani, NC, Maghsoud, Y, Hosseini, M, Babaei, A, Rahmani, H, Roe, SM, Gholivand, K. 2020. A new class of copper(I) complexes with imine-containing chelators which show potent anticancer activity. *Applied Organometallic Chemistry*; 34(8): 5526.
6. Gupta, RK, Sharma, G, Pandey, R, Kumar, A, Koch, B, Li, PZ, Xu, Q, Pandey, DS. 2013. DNA/Protein Binding, Molecular Docking, and in Vitro Anticancer Activity of Some Thioether-Dipyrinato Complexes. *Inorganic Chemistry*; 52(24): 13984-13996.
7. Asadi, Z, Zarei, L, Golchin, M, Skorepova, E, Eigner, V, Amirghofran, Z. 2020. A novel Cu(II) distorted cubane complex containing Cu<sub>4</sub>O<sub>4</sub> core as the first tetranuclear catalyst for temperature dependent oxidation of 3,5-di-tert-butyl catechol and in interaction with DNA&protein (BSA). *Spectrochimica Acta Part A: Molecular and Biomolecular Spectroscopy*; 227: 117593.
8. Bhunia, A, Vojtisek, P, Bertolasi, V, Manna, SC. 2019. Tridentate Schiff base coordinated trigonal bipyramidal/square pyramidal copper(II) complexes: Synthesis, crystal structure, DFT/TD-DFT calculation, catecholase activity and DNA binding. *Journal of Molecular Structure*; 1189: 94-101.
9. Kiraz, S, İnci, D, Aydın, R, Vatan, Ö, Zorlu, Y, Cavaş, T. 2019. Antiproliferative activity of copper(II) glutamine complexes with N,N donor ligands: Synthesis, characterization, potentiometric studies and DNA/BSA interactions. *Journal of Molecular Structure*; 1194: 245-255.
10. Balakrishnan, N, Haribabu, J, Dhanabalan, AK, Swaminathan, S, Sun, S, Dibwe, DF, Bhuvanesh, N, Awale, S, Karvemu, R. 2020. Thiosemicarbazone(s)-anchored water soluble mono- and bimetallic Cu(II) complexes: Enzymes-like activities, biomolecular interactions, anticancer property and real-time live cytotoxicity. *Dalton Transactions*; 49(22): 9411-9424.
11. Amitha, GS, Vasudevan, S. 2020. DNA binding and cleavage studies of novel Betti base substituted quaternary Cu(II) and Zn(II) phthalocyanines. *Polyhedron*; 190: 114773.
12. Liu, MC, Lin, TC, Sartorelli, AC. 1992. Synthesis and antitumor activity of amino derivatives of pyridine-2-carboxaldehyde thiosemicarbazone. *Journal of Medicinal Chemistry*; 35(20): 3672-3677.
13. Zarei, L, Asadi, Z, Samolova, E, Dusek, M, Amirghofran, Z. 2020. Pyrazolate as bridging ligand in stabilization of self-assembled Cu(II) Schiff base complexes: Synthesis, structural investigations, DNA/protein (BSA) binding and growth inhibitory effects on the MCF7, CT-26, MDA-MB-231 cell lines. *Inorganica Chimica Acta*; 509: 119674.
14. Bhunia, A, Mistri, S, Manne, RK, Santra, MK, Manna, SC. 2019. Synthesis, crystal structure, cytotoxicity study, DNA/protein binding and molecular docking of dinuclear copper(II) complexes. *Inorganica Chimica Acta*; 491: 25-33.
15. Kumar, P, Gorai, S, Santra, MK, Mondal, B, Manna, D. 2012. DNA binding, nuclease activity and cytotoxicity studies of Cu(II) complexes of tridentate ligands. *Dalton Transactions*; 41(25): 7573-7581.
16. Lu, JJ, Bao, JL, Wu, GS, Xu, WS, Huang, MQ, Chen, XP, Wang, YT. 2013. Quinones Derived from Plant Secondary Metabolites as Anti-cancer Agents. *Anti-Cancer Agents in Medicinal Chemistry*; 13(3): 456-463.
17. Rahman, AJ, Sharma, D, Kumar, D, Pathak, M, Singh, A, Kumar, V, Chawla, R, Ojha, H. 2021. Spectroscopic and molecular modelling study of binding mechanism of bovine serum albumin with phosmet. *Spectrochimica Acta Part A: Molecular and Biomolecular Spectroscopy*; 244: 118803.
18. Mo, D, Shi, J, Zhao, D, Zhang, Y, Guan, Y, Shen, Y, Bian, H, Huang, F, Wu, S. 2021. Synthesis and characterization of Fe<sup>III</sup>/Co<sup>III</sup>/Cu<sup>I</sup> complexes with Schiff base ligand and their hybrid proteins, SOD activity and asymmetric catalytic oxidation of sulfides. *Journal of Molecular Structure*; 1223: 129229.
19. Rani, JJ, Jayaseeli, AMI, Rajagopal, S, Seenithurai, S, Chai, JD, Raja, JD, Rajasekaran, R. 2021. Synthesis, characterization, antimicrobial, BSA binding, DFT calculation, molecular docking and cytotoxicity of Ni(II) complexes with Schiff base ligands. *Journal of Molecular Liquids*; 328: 115457.

20. Akgemci, EG, Saf, AO, Tasdemir, HU, Türkkan, E, Bingol, H, Turan, SO, Akkiprik, M. 2015. Spectrophotometric, voltammetric and cytotoxicity studies of 2-hydroxy-5-methoxyacetophenone thiosemicarbazone and its N(4)-substituted derivatives: A combined experimental-computational study. *Spectrochimica Acta Part A: Molecular and Biomolecular Spectroscopy*; 136: 719-725
21. Türkkan, E, Sayin, U, Erbilin, N, Pehlivanoglu, S, Erdogan, G, Tasdemir, HU, Saf, AO, Guler, L, Akgemci, EG. 2017. Anticancer, antimicrobial, spectral, voltammetric and DFT studies with Cu(II) complexes of 2-hydroxy-5-methoxyacetophenone thiosemicarbazone and its N(4)-substituted derivatives. *Journal of Organometallic Chemistry*; 831: 23-35.
22. Beckford, FA, Thessing, J, Shalowski, Jr M, Mbarushimana, PC, Brock, A, Didion, J, Woods, J, Gonzalez-Sarrias, A, Seeram, NP. 2011. Synthesis and characterization of mixed-ligand diimine-piperonal thiosemicarbazone complexes of ruthenium(II): Biophysical investigations and biological evaluation as anticancer and antibacterial agents. *Journal of Molecular Structure*; 992: 39-47.
23. Ishaq, M, Taslimi, P, Shafiq, Z, Khan, S, Salmas, RE, Zangeneh, MM, Saeed, A, Zangeneh, A, Sadeghian, N, Asari, A, Mohamad, H. 2020. Synthesis, bioactivity and binding energy calculations of novel 3-ethoxysalicylaldehyde based thiosemicarbazone derivatives. *Bioorganic Chemistry*; 100: 103924.
24. Zhang, X, Li, S, Yang, L, Fan, C. 2007. Synthesis, characterization of Ag(I), Pd(II) and Pt(II) complexes of a triazine-3-thione and their interactions with bovine serum albumin. *Spectrochimica Acta Part A: Molecular and Biomolecular Spectroscopy*; 68(3): 763-770.
25. Huseynovaa, M, Farzaliyev, V, Medjidov, A, Aliyeva, M, Taslimi, P, Sahin, O, Yalçın, B. 2020. Novel zinc compound with thiosemicarbazone of glyoxylic acid: Synthesis, crystal structure, and bioactivity properties. *Journal of Molecular Structure*; 1200: 127082.
26. Balakrishnan, N, Haribabu, J, Krishnan, DA, Swaminathan, S, Mahendiran, D, Bhuvanesh, NSP, Karvembu, R. 2019. Zinc(II) complexes of indole thiosemicarbazones: DNA/protein binding, molecular docking and in vitro cytotoxicity studies. *Polyhedron*; 170: 188-201.
27. Kalaierasi, G, Umadevi, C, Shanmugapriya, A, Kalaivani, P, Dallemer, F, Prabhakaran, R. 2016. DNA(CT), protein(BSA) binding studies, anti-oxidant and cytotoxicity studies of new binuclear Ni(II) complexes containing 4(N)-substituted thiosemicarbazones. *Inorganica Chimica Acta*; 453: 547-558.
28. Kılıç-Cıkla, I, Güveli, S, Yavuz, M, Bal-Demirci, T, Ülküseven, B. 2016. 5-Methyl-2-hydroxy-acetophenone-thiosemicarbazone and its nickel(II) complex: Crystallographic, spectroscopic (IR, NMR and UV) and DFT studies. *Polyhedron*; 105: 104-114.
29. Arafath, MA, Adam, F, Razali, MR, Ahmed Hassan, LE, Ahamed, MBK, Majid, AMSA. 2017. Synthesis, characterization and anticancer studies of Ni(II), Pd(II) and Pt(II) complexes with Schiff base derived from N-methylhydrazinecarbothioamide and 2-hydroxy-5-methoxy-3-nitrobenzaldehyde. *Journal of Molecular Structure*; 1130: 791-798.
30. Mathews, NA, Jacob, JM, Begum, PMS, Kurup, MRP. 2020. Cu(II) and Zn(II) complexes from a thiosemicarbazone derivative: Investigating the intermolecular interactions, crystal structures and cytotoxicity. *Journal of Molecular Structure*; 1202: 127319.
31. Nyawade, EA, Sibuyi, NRS, Meyer, M, Lalancette, R, Onani, MO. 2021. Synthesis, characterization and anticancer activity of new 2-acetyl-5-methyl thiophene and cinnamaldehyde thiosemicarbazones and their palladium(II) complexes. *Inorganica Chimica Acta*; 515: 120036.
32. Jacob, JM, Kurup, MRP, Nisha, K, Serdaroglu, G, Kaya, S. 2020. Mixed ligand copper(II) chelates derived from an O, N, S- donor tridentate thiosemicarbazone: Synthesis, spectral aspects, FMO, and NBO analysis. *Polyhedron*; 189: 114736.
33. Omondi, RO, Ojwach, SO, Jagany, D. 2020. Review of comparative studies of cytotoxic activities of Pt(II), Pd(II), Ru(II)/(III) and Au(III) complexes, their kinetics of ligand substitution reactions and DNA/BSA interactions. *Inorganica Chimica Acta*; 512: 119883.
34. Ayyannan, G, Mohanraj, M, Gopiraman, M, Uthayamalar, R, Raja, G, Bhuvanesh, N, Nandhakumar, R, Jayabalakrishnan, C. 2020. New Palladium(II) complexes with ONO chelated hydrazine ligand: Synthesis, characterization, DNA/BSA interaction, antioxidant and cytotoxicity. *Inorganica Chimica Acta*; 512: 119868.
35. Bağda, E, Yabas, E, Bağda, E. 2017. Analytical approaches for clarification of DNA double decker phthalocyanine binding mechanism: as an alternative anticancer chemotherapeutic. *Spectrochimica Acta Part A: Molecular and Biomolecular Spectroscopy*; 172: 199-204.
36. Bashiri, M, Jarrahpour, A, Nabavizadeh, SM, Karimian, S, Rastegari, B, Haddadi, E, Turos, E. 2021. Potent antiproliferative active agents: novel bis Schiff bases and bis spiroβ-lactams bearing isatin tethered with butylene and phenylene as spacer and DNA/BSA binding behavior as well as studying molecular docking. *Medicinal Chemistry Research*; 30: 258-284.
37. Kalantari, R, Asadi, Z. 2020. DNA/BSA binding of a new oxovanadium (IV) complex of glycyglycine derivative Schiff base ligand. *Journal of Molecular Structure*; 1219: 128664.
38. Tyagi, N, Singh, O, Mishra, RK, Ghosh, K. 2020. Bio-macromolecular interaction studies: Synthesis, crystal structure of water-soluble manganese(II) complexes. *Inorganica Chimica Acta*; 512: 119882.
39. Lakowicz, JR. Principles of fluorescence spectroscopy. New York: Springer Science & Business Media, 2013.
40. Shanmugapriya, A, Dallemer, F, Prabhakaran, R. 2018. Synthesis, characterisation, crystal structures and biological studies of palladium(II) complexes containing 5-(2-hydroxy-3-methoxyphenyl)-2,4-dihydro[1,2,4]triazole-3-thione derivatives. *New Journal of Chemistry*; 42(23): 18850-18864.
41. Haribabu, J, Sabapathi, G, Tamizh, MM, Balachandran, C, Bhuvanesh, NSP, Venuvanalingam, P, Karvembu, R. 2018. Water-Soluble Mono- and Binuclear Ru(η<sup>6</sup>-p-cymene) Complexes Containing Indole Thiosemicarbazones: Synthesis, DFT Modeling, Biomolecular Interactions, and In Vitro Anticancer Activity through Apoptosis. *Organometallics*; 37(8): 1242-1257.
42. Feng, XZ, Lin, Z, Yang, LJ, Wang, C, Bai, CL. 1998. Investigation of the interaction between acridine orange and bovine serum albumin. *Talanta*; 47(5): 1223-1229.
43. Abdel-Rahman, LH, Abu-Dief, AM, Moustafa, H, Hamdan, SK. 2017. Ni(II) and Cu(II) complexes with ONNO asymmetric tetradentate Schiff base ligand: synthesis, spectroscopic characterization, theoretical calculations, DNA interaction and antimicrobial studies. *Applied Organometallic Chemistry*; 31(2): e3555.
44. Palmucci, J, Mahmudov, KT, Guedes da Silva, MFC, Marchetti, F, Pettinari, C, Petrelli, D, Vitali, LA, Quassinti,



- L, Bramucci, M, Lupidi, G, Pombeiro, AJL. 2016. DNA and BSA binding, anticancer and antimicrobial properties of Co(ii), Co(ii/iii), Cu(ii) and Ag(i) complexes of arylhydrazones of barbituric acid. *RSC Advances*; 6: 4237-4249.
45. Sedighipoor, M, Kianfar, AH, Mahmood, WAK, Azarian, MH. 2017. Synthesis and electronic structure of novel Schiff bases Ni/Cu (II) complexes: Evaluation of DNA/serum protein binding by spectroscopic studies. *Polyhedron*; 129: 1-8.
46. Khan, A, Paul, K, Singh, I, Jasinski, JP, Smolenski, VA, Hotchkiss, EP, Kelley, PT, Shalit, ZA, Kaur, M, Banerjee, S, Royd, P, Sharma, R. 2020. Copper(I) and silver(I) complexes of anthraldehyde thiosemicarbazone: synthesis, structure elucidation, in vitro anti-tuberculosis/cytotoxic activity and interactions with DNA/HSA. *Dalton Transaction*; 49: 17350-17367.